

# Additive Manufacturing-Enabled Low-Cost Particle Detector

Tanja Wallner<sup>1,2</sup>, Markus Bainschab<sup>1</sup>, Reinhard Klambauer<sup>2</sup>, Alexander Bergmann<sup>2</sup>

<sup>1</sup> Silicon Austria Labs <sup>2</sup> Graz University of Technology

## Corresponding Author

Tanja Wallner

tanja.wallner@silicon-austria.com

## Citation

Wallner, T., Bainschab, M., Klambauer, R., Bergmann, A. Additive Manufacturing-Enabled Low-Cost Particle Detector. *J. Vis. Exp.* (193), e64844, doi:10.3791/64844 (2023).

## Date Published

March 24, 2023

## DOI

10.3791/64844

## URL

jove.com/video/64844

## Abstract

As particles with a size of 1  $\mu\text{m}$  or smaller pose a severe health risk to the human body, the detection and regulation of particle emissions are of great importance. A large share of particulate emissions are emitted by the transport sector. Most of the commercially available particle detectors are bulky, very expensive, and need additional equipment. This paper presents a protocol to build and test a standalone particle detector that is small and cost-efficient.

The focus of this paper lies in the description of the detailed construction manual with video and the sensor evaluation procedure. The computer-aided design model of the sensor is included in the supplemental material. The manual explains all the construction steps, from 3D printing to the fully operational sensor. The sensor can detect charged particles and is therefore suitable for a wide range of applications. A possible field of application would be soot detection from power plants, wildfires, industries, and automobiles.

## Introduction

Inhalation of particles with a size of 1  $\mu\text{m}$  or smaller poses a high risk of adverse health effects on the human body. With increasing environmental pollution from combustion processes, respiratory diseases are growing in the population<sup>1,2,3</sup>. To promote health and counteract pollution, it is necessary to first identify the sources of pollution and quantify the degree of pollution. This can be done with

existing particle detectors. However, these are large and very often far too expensive for private or citizen science purposes.

Many of the commercially available particle detectors are bulky, very expensive, and require additional equipment to be operated<sup>4</sup>. Most of them also need several aerosol-conditioning steps. For example, dilution is needed for detectors that use light scattering as their measurement principle, and the measurement range is limited by the wavelength<sup>5,6,7</sup>. Particle detectors that use laser-induced

incandescence as a detection principle need both high energy laser sources and an energy-consuming cooling system<sup>8</sup>.

Particle detectors that use condensation particle counters are normally used as the gold standard for particle concentration measurement; these need preconditioning, dilution, and working fluids (e.g., butanol)<sup>9,10,11</sup>. The advantages of an electrostatic sensor lie in the simple and compact design and the low fabrication costs. However, in comparison to condensation particle counters, significant deductions have to be made regarding accuracy.

An electrostatic sensor represents an alternative to these methods. Electrostatic sensors can be robust, light, inexpensive to manufacture, and can be operated without supervision. The simplest form of an electrostatic sensor is a parallel plate capacitor with a high electric field between its plates. As aerosol is conveyed into the high voltage region between the two copper electrodes, naturally charged particles deposit on the electrodes of different polarity<sup>12</sup> (**Figure 1**).

Dendrites form on the surface of the electrodes in the direction of the field lines of the applied high voltage between the electrodes, and are charged *via* contact charging. Fragments of these dendrites eventually break off the electrodes and redeposit on the electrode with opposite polarity, transferring their charge. These fragments carry a high number of charges. Because the electrode is grounded, the deposited charge generates a current leading to a voltage drop at the internal resistance of the bench multimeter. The more often this happens per unit of time, the higher the current, and consequently, the higher the voltage drop (**Figure 2**).

Owing to the high voltage induced by the charge deposition of the fragments, no further amplifier electronics are needed. The formation of dendrite break-off particles and the subsequent charge release of these particles represents a natural signal amplification<sup>12</sup>. The resulting sensor signal is proportional to the particle mass concentration. This signal can be detected with an off-the-shelf bench multimeter.

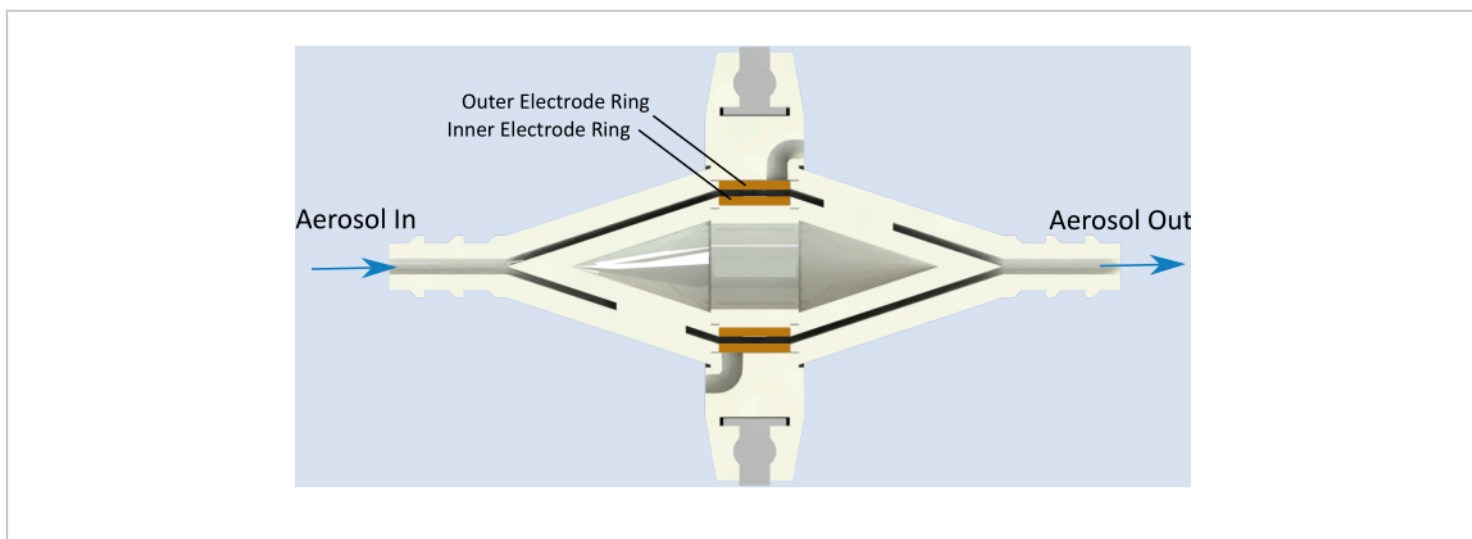


**Figure 1: Sensor schematics.** Aerosol flows into the aerosol inlet, is propagated through the left flow channel, and then reaches the gap between the high-voltage electrode (inner electrode) and the measuring electrode (outer electrode). There,

the particles contribute to dendrite growth and, as previously explained, break-off, thus generating the sensor response. Afterward, the particles flow further through the right flow channel and leave the sensor at the aerosol outlet. [Please click here to view a larger version of this figure.](#)

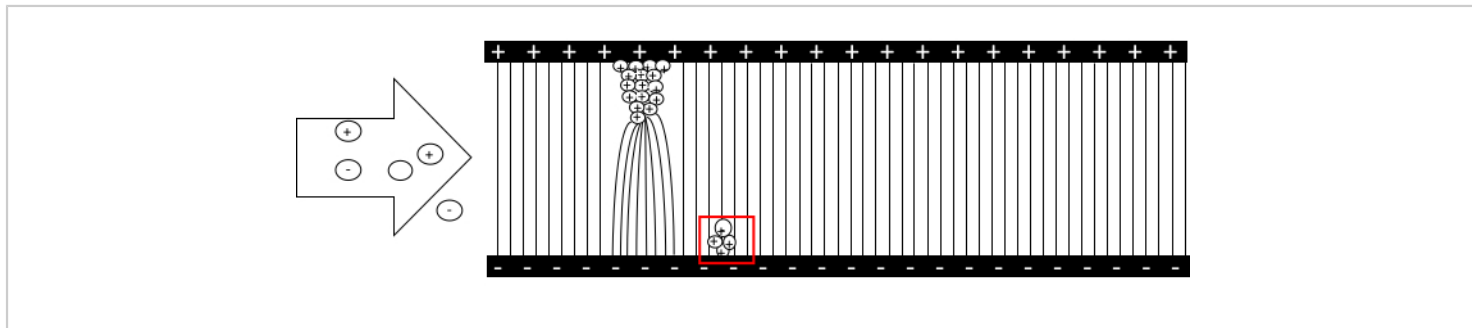


**Figure 2: Physical principle.** Positively and negatively charged particles, as well as neutral particles, enter the gap between the electrodes of opposite polarity. They are diverted by the electric field lines to the electrode of opposite polarity and deposit their charge there. Then, they become part of a dendrite and take over the charge of the respective electrode. The field density is highest at the dendrite tip, where more particles are trapped. When the drag force exceeds the binding forces, segments of the dendrites break off, which in turn strike the opposite electrode and deposit their charges. [Please click here to view a larger version of this figure.](#)

With a cylindrical design, as in Warey et al.<sup>10</sup>, the probability of soot bridges forming can be minimized. Further information about the sensor geometry, applied voltage, gas flow velocity, and particulate matter concentration can be found there. They suggest correlation of the sensor signal to particulate matter streaming through the sensor (equation 1).

$$\text{Sensor (V)} = 5.7 \times 10^{-5} C V_0 e^{0.62V} \times \frac{L}{S^{1.28}} \quad (1)$$

C is the mass concentration of the particulate matter,  $V_0$  is the applied voltage, V is the exhaust velocity, L is the electrode length, and S is the electrode gap<sup>13</sup>.

Bilby et al. focused on the detailed study of the underlying physical effect of the electrostatic sensor<sup>9</sup>. These studies included an optically accessible setup and a kinetic model to

explain the signal amplification of the dendrite-based sensor (see equations 2 and 3).

$$\frac{d[D_n]}{dt} = k_s[S] ([D_{n-1}] - [D_n]) + k_{n+f} [D_{n+f}] - k_n[D_n] + k_b[Br] ([D_{n-f}] - [D_n]) \quad (2)$$

$$\frac{d[Br]}{dt} = \sum_{i=f}^{\infty} k_i[D_i] - k_b[Br] \sum_{i=0}^{\infty} [D_i] - k_L [Br] \quad (3)$$

S represents a stack of soot discs of 10-100 soot agglomerates with a size of 50-100 nm;  $D_n$  represents a dendrite with n disks; Br denotes a break-off fragment composed of f disks; S and  $k_i$  are rate constants<sup>12</sup>.

This paper presents a protocol on how to build and test a simple but efficient low-cost particle detector that can be used for high particle concentrations without further equipment. Previous work on this type of electrostatic sensor has mostly focused on exhaust measurements. In this work, laboratory-generated soot particles are used as test aerosols. The

described sensor is based on previous work from Waley et al. and Bilby et al<sup>12,13</sup>.

The sensor body consists of a stereolithography-based 3D printed body, coaxial electrodes cut from copper tubes, a vacuum gasket, and a vacuum clamp. Materials such as the vacuum gasket, cable, copper tubes, and 3D resin for one sensor cost less than €40. The additional equipment needed is a high-voltage source, a USB bench multimeter, and a soldering station. To evaluate the sensor, a defined aerosol source and a reference instrument are also required once

(see **Table of Materials**). The size of the sensor described in this protocol is 10 cm x 7 cm. This size was chosen specifically for the experiment and can still be reduced significantly (see modifications/sensor dimensions in the discussion).

This protocol describes how to build, test, and use a simple low-cost particle sensor. A schematic of the protocol is shown in **Figure 3**-beginning with the 3D print of the sensor hull and the electrode manufacturing, the assembly of the sensor, as well as testing and an example of field application of the sensor.

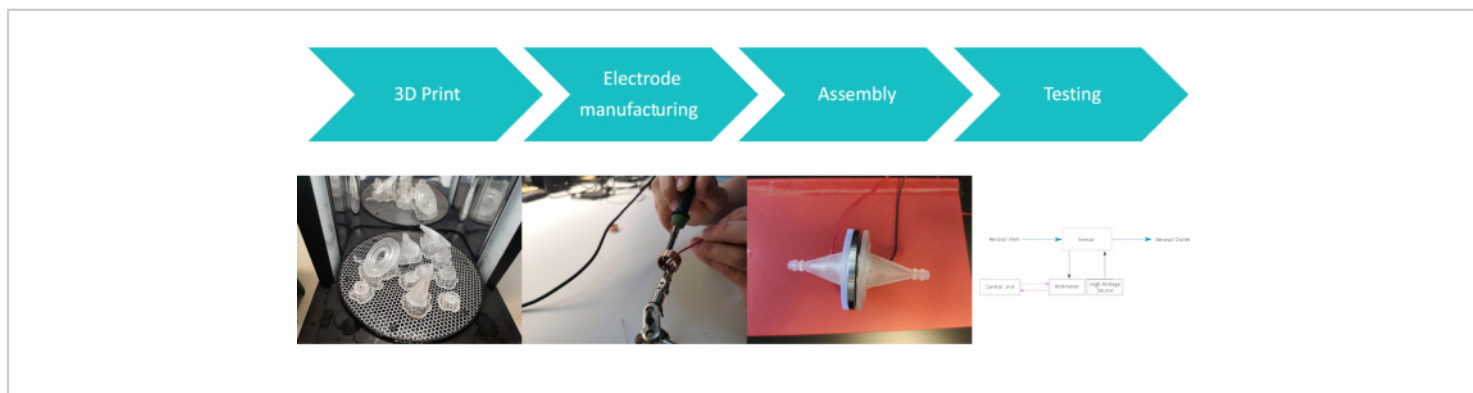


**Figure 3: Schematic for the method.** The protocol is divided into four major steps. First, all parts for the sensor housing are printed. Then, the electrodes are manufactured. In the third step, the 3D printed sensor housing with the electrodes and the vacuum gasket are assembled. In the last step, the sensor performance is evaluated. [Please click here to view a larger version of this figure.](#)

The most important steps of the 3D printing process are shown in **Figure 4**. At first, the right slicer settings for the print are chosen. Afterward, the most important parts of the print

and the preprocessing of the 3D printed model are discussed. For this step, a resin 3D printer with an isopropanol bath and UV hardening device and a straight grinder are needed.

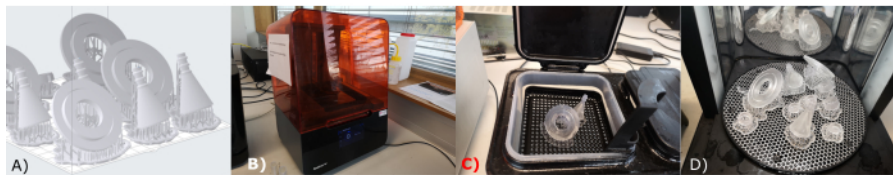


**Figure 4: Schematic of 3D print.** (A) The slicer 3D model is depicted; (B) the printer during the printing process. Postprocessing steps: (C) flushing and (D) UV-hardening. [Please click here to view a larger version of this figure.](#)

**Figure 5** shows the most important steps of electrode manufacturing: the form shaping of the electrodes as well as the soldering of the contact to the electrodes. For this step, two copper tubes with different diameters, a caliper, a

pipe cutter, a straight grinder, a vice, a soldering station and soldering tin, isolated cables with two different colors, thermal protective gloves, and a wire cutter are needed.

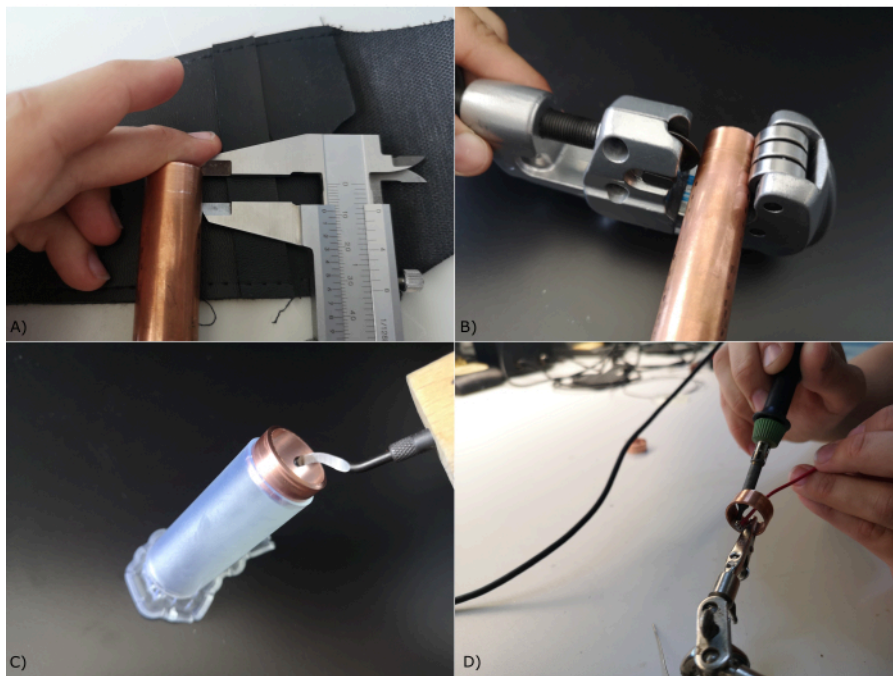


**Figure 5: Electrode manufacturing.** (A) Measuring, (B) cutting, (C) deburring, and (D) soldering of the electrodes. [Please click here to view a larger version of this figure.](#)

The assembly section in the protocol explains how the sensor is assembled. The most important sensor parts are depicted

in **Figure 6**, namely the outer electrode holder, the flow channel, and the inner electrode holder. **Figure 7** shows the

most important steps in the sensor assembly. For this step, epoxy glue, protective clothing, a vacuum seal, a vacuum clamp, safety goggles, and gloves are needed.

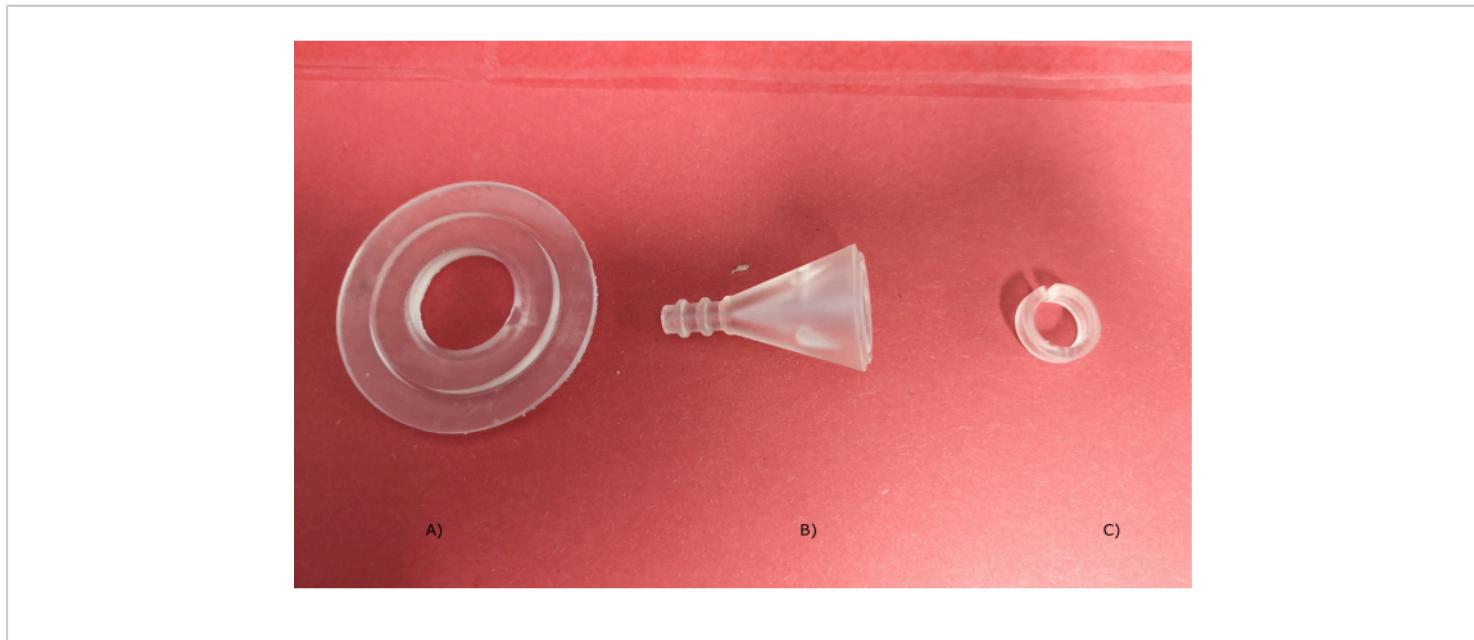


**Figure 6: Sensor parts.** (A) The outer electrode holder, (B) flow channel, and (C) the inner electrode holder. [Please click here to view a larger version of this figure.](#)

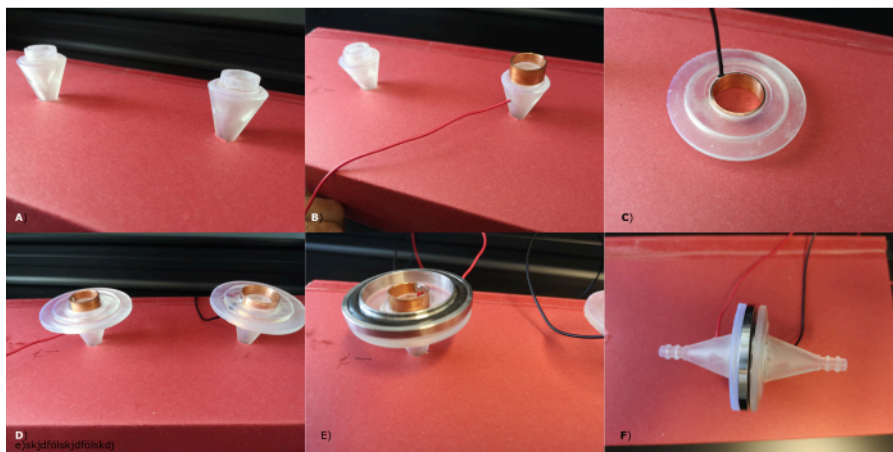


**Figure 7: Sensor assembly.** All steps of the sensor assembly are shown. **A-E** shows the assembly of one half of the sensor. **(A)** The inner electrode holder is glued to the flow channel. **(B)** The inner electrode is placed onto the inner electrode holder. **(C)** The outer electrode is placed into the outer electrode holder. **(D)** The outer electrode holder is glued onto the flow channel + inner electrode holder assembly. **(E)** The vacuum sealing snaps into the outer electrode of one sensor half and then snaps into **(C)**, the identical second outer electrode of the other sensor half. [Please click here to view a larger version of this figure.](#)

The test section explains how to set up the experiment to compare the newly built sensor with a reference instrument. For this step, a bench multimeter, vacuum pump, high-voltage supply, aerosol generator, dilution bridge, aerosol tubes, Y-fitting, one mass flow controller (MFC), an aerosol mixer, a reference instrument, and a cotton swab are needed.

## Protocol

### 1. 3D printing

#### 1. Slicer settings

1. Open all ".stl" files with the slicer software and place the sensor parts on the platform (see **Supplemental File 1, Supplemental File 2, Supplemental File 3,**

#### **Supplemental File 4, Supplemental File 5, and Supplemental File 6).**

2. For a good printing result, tilt all the parts with respect to the platform.
  3. Generate support points with a **density of 0.8** and a **point size of 0.4 mm**.
  4. Select **Clear V4** with a **layer thickness of 50  $\mu\text{m}$** .
2. Start printing.
    1. Upload the slicer output file on the 3D printer.
    2. Look for the printing time and resin volumes that are displayed on the screen. Insert the clear V4 tank and resin cartridge, attach the mounting platform, and open the cartridge lid. Press **Start** on the printer.
  3. Immediate post-processing

1. After the print is finished, open the printer and detach the mounting platform.  
**NOTE:** This step can only be delayed if it is sure that the model will stay under the UV protection screen of the printer (see critical steps/print post-processing in the discussion).
  2. Gently peel all parts from the platform and place them in an isopropanol bath.
  3. Move the parts constantly for 20 min.
  4. Take out the parts every 5 min and flush all small gaps and holes thoroughly.
4. UV-hardening
1. Dry the parts before starting the hardening process.
  2. Flush all small gaps and holes with pressurized air.
  3. Place the parts into the UV hardening device and harden them for 50 min at 40 °C.  
**NOTE:** This setting differs from the manufacturer's recommended drying time and temperature (see critical steps/print post-processing in the discussion).
5. Post-processing
1. Check that all the cavities and holes are open.
  2. If a path is clogged, drill or scrape it with the straight grinder.
  3. Check that all the printed parts fit properly and that the copper tubes can be inserted. If they can't, then sand them down.

## 2. Electrode manufacturing

1. Measure 9 mm from the top of the 18 mm and 22 mm copper pipes and mark these positions.

2. Cut the pipes with the pipe cutter at the markings.  
**NOTE:** Make sure not to use too much force during the process. It takes several turns to cut through the pipes (see critical steps/electrode manufacturing in the discussion section).
  3. Deburr the copper ring carefully. Do not put too much pressure on the copper ring while deburring and try not to scratch the electrode surface.  
**NOTE:** This is a very critical part and affects the performance of the sensor (see critical steps/electrode manufacturing and modifications/electrodes in the discussion section).
4. Electrode soldering
1. Solder the red cable to the inner copper ring (18 mm) and the black cable to the outer copper ring (22 mm).
  2. Polish the copper ring to get rid of the oxidized copper layer on the surface.
  3. Clamp the ring in a vice.
  4. Pre-tin both the copper ring and the cable and solder the cable to the ring.  
**CAUTION:** Due to the soldering, the copper electrodes heat up to 400 °C. Only touch the electrodes with tweezers and wear thermo-protective gloves.

## 3. Assembly

1. Mix the two components of the epoxy glue in a tray.  
**NOTE:** It is very important to use transparent glue to differentiate between soot bridges and hardened glue.  
**CAUTION:** Work under a fume hood, wear protective clothes (especially gloves), and clean work surfaces. Further safety instructions can be found in the safety data

sheet. Health hazard: "Skin Corr. 1C - H314 Eye Dam. 1 - H318 Skin Sens. 1 - H317".

2. Stick the inner electrode holder into the flow channel and wait 60 min for the glue to harden (**Figure 7A**).
3. Place the inner electrode ring (18 mm) on the holder and guide the cable through the cable channel (**Figure 7B**).  
**NOTE:** Make sure that there is enough space for the soldering point.
4. Place the spacer around the inner electrode.  
**NOTE:** This is a very critical step. If the distance between the electrodes is not exactly 1 mm everywhere in the entire sensor, the electric field, and subsequently the sensor performance, can be influenced (see critical steps/electrode manufacturing in the discussion).
5. Place the outer electrode ring (22 mm) on the holder and feed the cable through the cable channel (**Figure 7C**).
6. Glue the outer electrode holder onto the flow channel. Insert the spacer into the gap between the two copper electrodes. Wait 60 min for the glue to harden (**Figure 7D**).
7. Seal all the cable channels with epoxy glue. Wait overnight for the glue to cure.
8. Insert the vacuum seal in the printed valve of the outer electrode. Insert the two sensor sides into each other and fasten them with the vacuum clamp (**Figure 7E,F**).

#### 4. Tests

1. Open the vacuum clamp of the sensor.
2. Pull the two halves of the sensor apart and remove the seal.

3. From there, touch the electrode ring with one multimeter probe tip, and the end of the cable leading to the electrode with the other multimeter tip.
4. Pretests
  1. Test the electrical connection of the electrode and the cable with the multimeter. Check whether the resistance is  $<2 \Omega$  (depending on the level of oxidation).
  2. Plug the hose onto the aerosol inlet and outlet and test if the sensor is airtight with the vacuum pump.
5. Parallel experiment
  1. Build the sensor setup, according to **Figure 8**.
    1. Connect the high-voltage power supply to the red sensor cable (high-voltage electrode).
    2. Connect the black sensor cable to the bench multimeter voltage input.
    3. Connect the electrometer ground (GND) with the power supply GND.
    4. Connect the multimeter USB cable to the PC.
  2. Incorporate the sensor into the aerosol measurement setup, according to **Figure 9**.
  3. Aerosol generator
    1. **Gas supplies:** Turn on the sheath flow, nitrogen, and propane supply (pressure needed: nitrogen, 4 bar; other gases, 1 bar each).
    2. **Power source:** Plug in the 24 V source cable for the built-in MFCs and connect the USB to the PC.
    3. **Software:** open the MFC software and insert the correct COM port number. Search for

devices: if five devices are displayed (for five different MFCs), click **stop searching**. Input the starting conditions according to the aerosol generator's user manual: **10 mL/min propane, 1.55 L/min oxidation air, 7 L/min quench gas, 20 L/min dilution air.**

4. Start the aerosol generator (see **Table of Materials**) by turning the **ON-OFF knob**. When the knob is turned on, the nitrogen indicator is on, indicating all flow paths are open. Hold the flame-safety device and press the **ignite button** on the aerosol generator; observe a flame in the combustion chamber window. Release the flame-safety device after ~60 s very slowly.
5. Enter the following mass flows: **60 mL/min propane, 1.55 L/min oxidation air, 7 L/min nitrogen (quench), and 20 L/min dilution air** to set the correct size distribution parameters.  
**CAUTION:** Connect the generator to the rest of the setup only if measurements are to be taken within the next minutes; otherwise, the filters of the dilution bridge will clog rapidly.
4. Connect the dilution bridge to the aerosol generator. Disconnect it once again and divert the aerosol flow to the fume hood until the start of the experiment. Make sure that the dilution bridge is closed before starting the experiment.
5. Connect the dilution bridge outlet to the aerosol mixer inlet.
6. Connect the aerosol mixer outlet 2 (see **Figure 9E**) to the sensor inlet.
7. Incorporate the MFC.

1. Connect a high-efficiency particulate absorbing (HEPA) filter to the sensor outlet and connect the sensor outlet to the MFC inlet.
2. Connect the power supply of the MFC and connect the USB to the PC.
8. Open the MFC software and input the correct COM port number.
  1. Search for devices.
  2. Click **stop searching?**
  3. Input the **mass flow** as **1 L/min**.
9. Reference instrument (see **Table of Materials**)
  1. Connect the LAN cable to the PC and open a connection to the IP address of the reference instrument in the browser to open a java application to control the reference instrument.
  2. In the reference instrument control software, press **lock resources | stand by** to start the pump.  
**NOTE:** The heating process takes ~20 min.
  3. After the warm-up phase, click **measurement** to measure the aerosol entering the reference instrument.
  4. Choose a **dilution ratio** of **1:10** on the reference instrument.
  5. Use a y-fitting to connect the aerosol mixer outlet 1 (see **Figure 9D**) and the dilution airflow to the split end of the y-fitting (see **Figure 9C**), and connect the single end of the y-fitting to the reference instrument inlet.  
**NOTE:** These two flows are then combined at the single end of the y-fitting.

## 10. Start of experiment

1. Connect the aerosol generator to the dilution bridge once again and make sure the dilution bridge is closed.
2. Click **measure** on the reference instrument.
3. Slowly open the dilution bridge until the desired aerosol mass concentration of **3-5 mg/m<sup>3</sup>** is reached, and start logging data on the reference instrument.
4. Observe the reference instrument particle mass concentration. When the aerosol source is stable, switch on the **sensor power supply** at **1,000 V** and start logging the data.

**NOTE:** If the concentration is not stable, see troubleshooting in the discussion section.

## 11. Collect data from the bench multimeter with a **read** command on the console or an automated script.

**NOTE:** After the sensor current stabilizes (approximately 5 min), a comparison of the reference instrument with the sensor current is possible.

**CAUTION:** If the sensor current increases rapidly above  $10^{-7}$  A (corresponding to 0.1 V with an internal resistance of 1 M $\Omega$ ), switch off the high voltage source (see troubleshooting in the discussion section).

## 12. Parallel measurement: After the sensor reaches equilibrium, measure a concentration gradient in steps from **5 mg/m<sup>3</sup>** to **0.2 mg/m<sup>3</sup>** by adjusting the dilution bridge accordingly.

**NOTE:** When higher concentrations are used, the dilution ratio of the reference instrument must be increased.

6. Clean the sensor with pressurized air and a swab before each new measurement.

## 5. Field application

1. Build the sensor setup, according to **Figure 8**.
  1. Connect the high-voltage power supply to the red sensor cable (high voltage electrode).
  2. Connect the black sensor cable to the bench multimeter voltage input.
  3. Connect the electrometer GND with the power supply GND.
  4. Connect the multimeter USB cable to the PC.
2. Incorporate the sensor setup into the new measurement setup, according to **Figure 10**, and connect the aerosol source with the sensor.
3. Split the outflowing particle stream from the aerosol source into path A) sensor setup and path B) ventilation.
  1. MFC or pump: Use an MFC to pass the sample through the sensor.
  2. Use a HEPA filter upstream of the MFC. Connect the power supply of the MFC and connect the USB to the PC.
  3. Follow step 4.5.8 for parallel measurement.
4. Start of field experiment: Make sure that the aerosol source is connected to the sensor input.
5. Switch on the sensor power supply and start logging data.

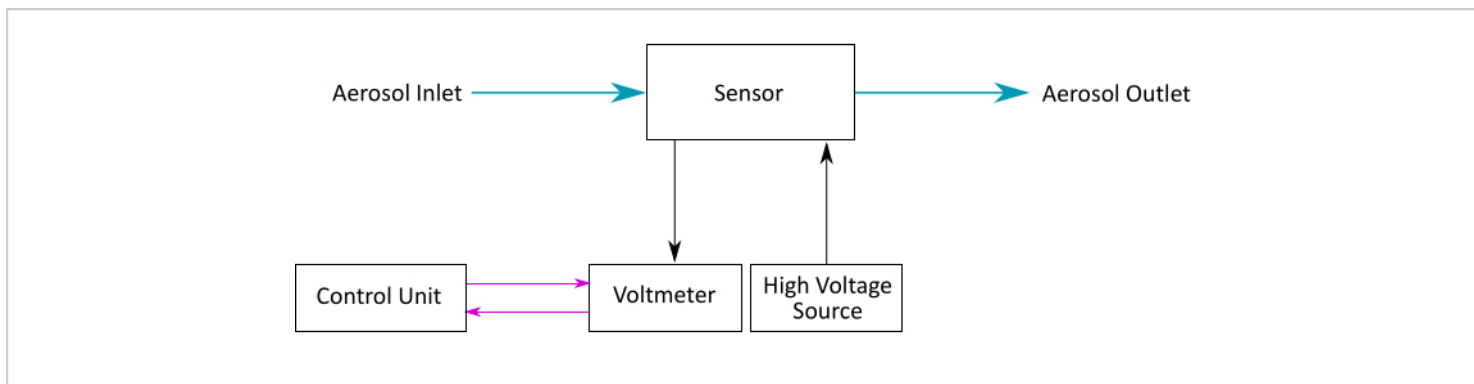


**Figure 8: Sensor setup.** A diagram of the sensor setup. Aerosol flows through the sensor. The sensor is connected to the voltmeter and a high-voltage supply. The voltmeter is controlled by a control unit that logs the sensor data. [Please click here to view a larger version of this figure.](#)

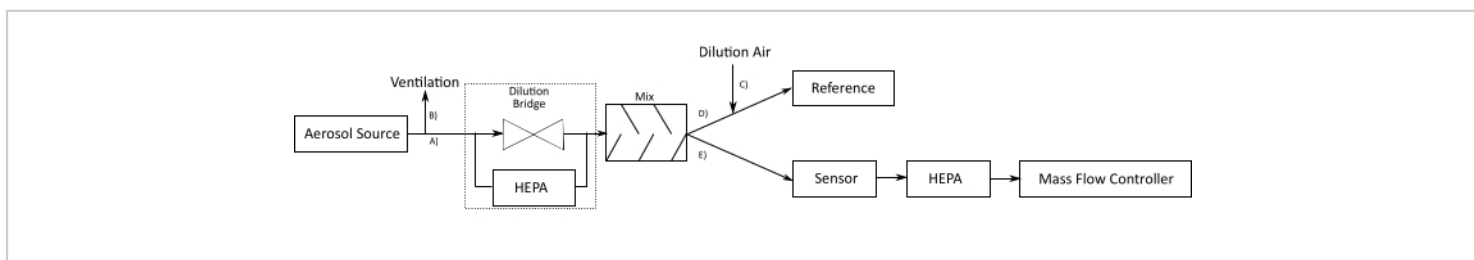


**Figure 9: Experimental plan for sensor evaluation.** A stable aerosol source is used to mimic a particle source. The outflowing particle stream is split into path (A), sensor setup; and path (B), ventilation, enters the dilution bridge, and is further distributed to an aerosol mixer. After the mixer, the aerosol stream is split between a reference instrument path (D), which measures parallel to the sensor. This reference instrument needs dilution air, which is distributed through path (C). Path (E): an MFC draws air through the sensor. This MFC is protected from the aerosol stream with a HEPA filter. Abbreviations: MFC = mass flow controller; HEPA filter = high-efficiency particle absorbing filter. [Please click here to view a larger version of this figure.](#)

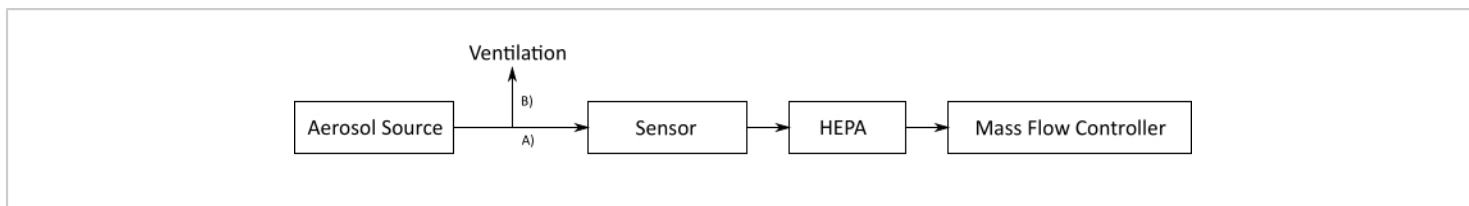


**Figure 10: Field test: the experimental plan.** In this setup, an aerosol source is measured. The outflowing particle stream is split into path A) sensor setup and path B) ventilation and then enters the sensor. In this setup, an MFC with a HEPA filter upstream sucks the aerosol through the sensor. Abbreviations: MFC = mass flow controller; HEPA filter = high-efficiency particle absorbing filter. [Please click here to view a larger version of this figure.](#)

## Representative Results

The exact correlation of the sensor signal to particulate mass varies based on particle charge distribution and size distribution, as well as the aerosol composition. Therefore, the sensor must be calibrated to a particular application with a reference instrument. This section explains how to compare the newly built sensor with a reference instrument.

The starting phase of the sensor takes approximately 5-10 min, depending on the chosen particle concentration. Within the starting phase, the sensor signal significantly increases while the sensor is exposed to a constant particle concentration. After the starting phase, the sensor signal stabilizes. At that stage, an equilibrium state for accumulation and fragmentation of dendrites is reached and the sensor signal is then proportional to the incoming soot concentration.

After this initialization phase, the sensor is ready to measure any changes in aerosol concentration.

The measurement data shown in **Figure 11** starts from the moment the sensor is in the above-mentioned equilibrium state. To calculate the sensor current in amperes, the collected data in volts must be divided by the value of internal resistance to obtain the correct current value.

The vertical axis shows the sensor signal in amperes and the horizontal axis shows the aerosol concentration measured by the reference instrument in  $\text{mg}/\text{m}^3$ . A linear fit with its representative parameters is also given in the plot. The high uncertainty of the measured data is due to the high dynamics when adjusting the concentration with the dilution bridge. The linear fit parameters are an  $R^2$  value of 0.80, an intercept of  $-0.53 \text{ nA}$ , and a slope of  $2.80 \text{ nAm}^3/\text{mg}$  with a standard deviation of  $1.4 \text{ nA}$ .

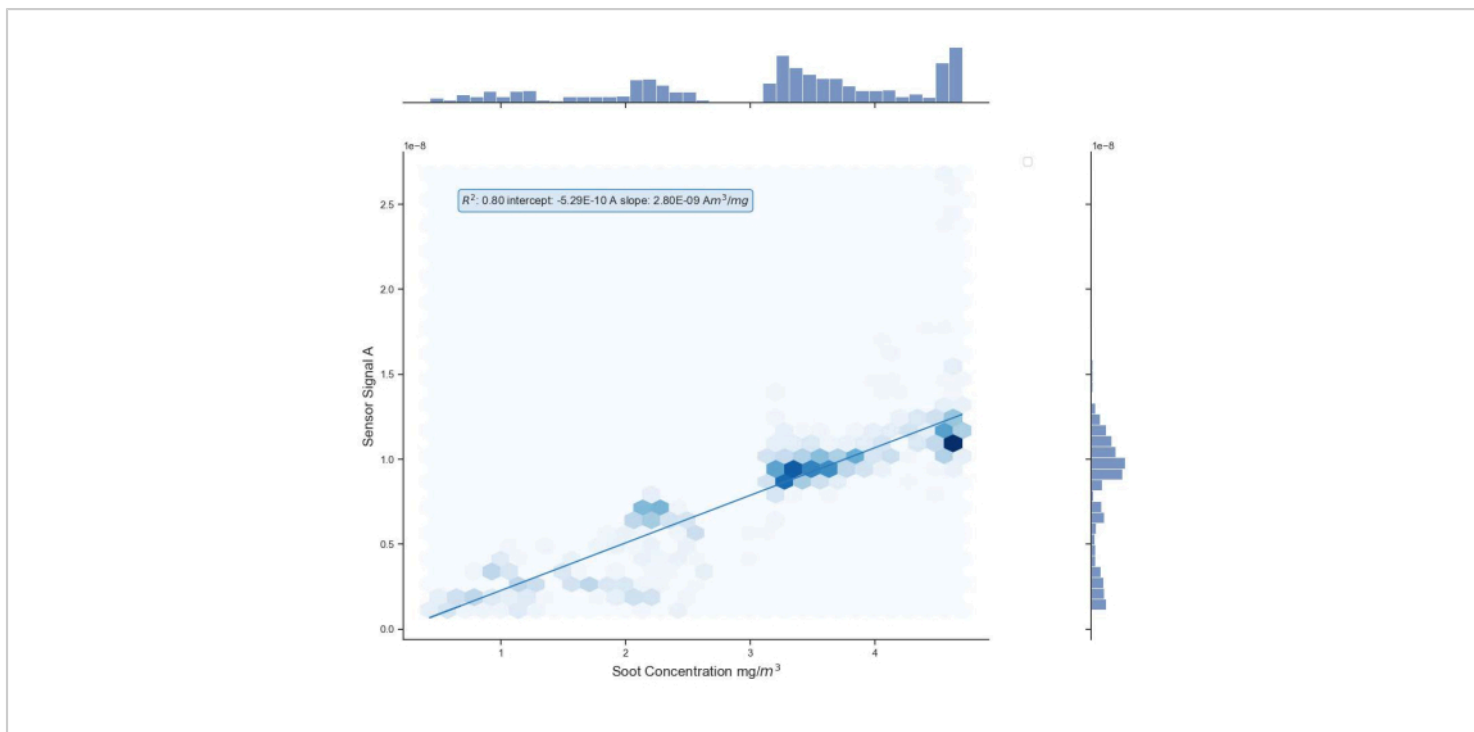


**Figure 11: Positive results.** The sensor signal is plotted on the vertical axis in amperes, whereas the particle concentration measured by the reference instrument in  $\text{mg}/\text{m}^3$  is plotted on the horizontal axis. In addition, a linear fit with the most important parameters is added to the plot. The linear fit parameters are an  $R^2$  value of 0.80, an intercept of  $-0.53 \text{ nA}$ , and a slope of  $2.80 \text{ nAm}^3/\text{mg}$ . [Please click here to view a larger version of this figure.](#)

There is also the possibility that particles clog the path between the electrodes, in which case conductive soot bridges form between the electrodes. Because soot is a conductive material, these soot bridges form a short circuit between the electrodes. The measured signal rises rapidly with increasing thickness of the conductive path, up to the point where the voltage becomes so high that the voltmeter

might be damaged. An example for an experiment with forming soot bridges can be seen in **Figure 12**. The signal rises in very steep jumps/steps and does not stop or flatten out. Dendrites are also no longer formed, and the sensor is no longer in a state of equilibrium. In this case, the high-voltage source must be switched off immediately, the sensor has to be cleaned, and a new measurement has to be started.

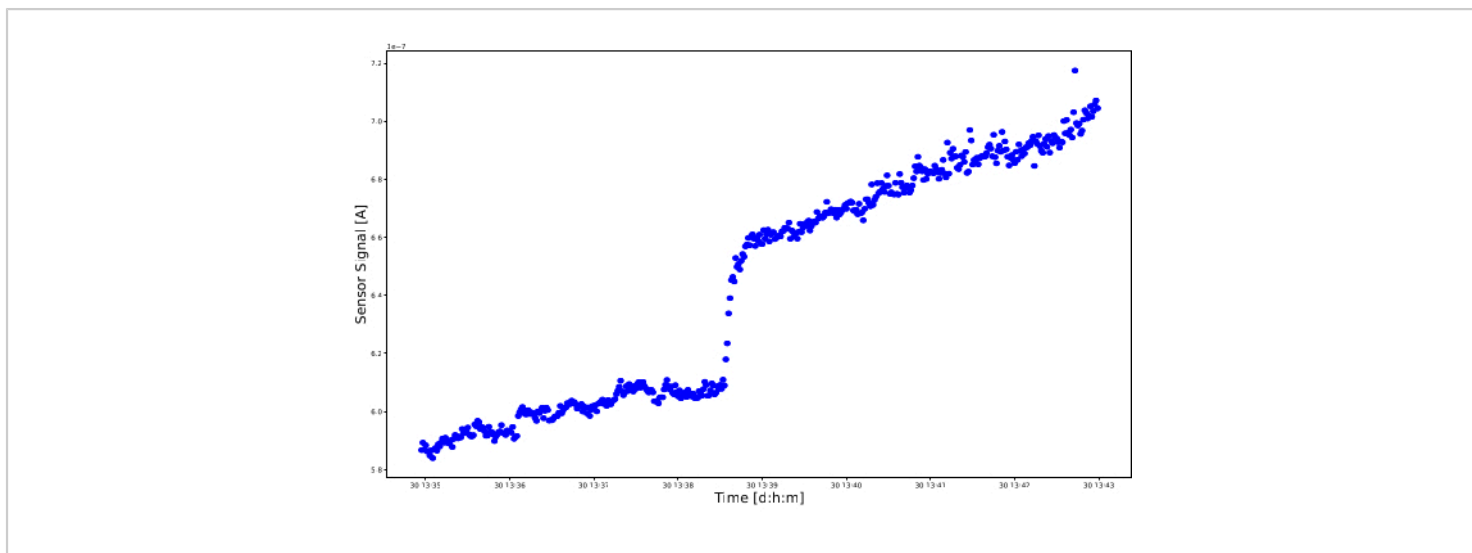


**Figure 12: Negative result.** A short circuit has occurred during the measurement. The sensor signal in amperes is plotted on the vertical axis and the measurement time is plotted on the horizontal axis. The sensor signal continues to increase without restriction. [Please click here to view a larger version of this figure.](#)

If a flat line is displayed and the sensor current does not rise at all to a value above 1 nA, follow the troubleshooting directions in the discussion section. The sensor must be in the equilibrium state at all times to measure the entering aerosol accurately; therefore, a sufficiently high initial aerosol concentration has to be provided at the beginning of the experiment.

**Supplemental File 1:** This file represents the computer-aided design (CAD) file to print out the flow channel depicted in Figure 7A with holes for the cable. [Please click here to download this File.](#)

**Supplemental File 2:** This file represents the CAD file to print out the flow channel depicted in Figure 7A without holes. [Please click here to download this File.](#)

**Supplemental File 3:** This file represents the CAD file to print out the inner electrode holder depicted in Figure 7A. [Please click here to download this File.](#)

**Supplemental File 4:** This file represents the CAD file to print out the outer electrode holder depicted in Figure 7C (right). [Please click here to download this File.](#)

**Supplemental File 5:** This file represents the CAD file to print out the flow channel without holes depicted in Figure 7C (left). [Please click here to download this File.](#)

**Supplemental File 6:** This file represents the CAD file to print out the electrode spacer. [Please click here to download this File.](#)

## Discussion

### Critical steps

*Print post-processing*

Almost any step in this protocol can be paused or postponed, except for post-processing of the freshly printed 3D parts (protocol step 1.5). If the UV protection screen of the printer is opened, the post-processing should begin immediately, otherwise the small cable channels, as well as the cavity for the seal, will clog. The precision fit of the cavity ensures that the sensor can be sealed airtight. This is important because the sensor is very sensitive to flow fluctuations. The hardening process is also important (protocol step 1.4); if the temperature is set too high, the material becomes too brittle and can break under the forces exerted by the clamp onto the outer electrode holder.

#### *Electrode manufacturing*

Careful cutting and deburring (protocol steps 2.2-2.3) of the electrodes is very important because irregularities in the electrode gap cause perturbations in the electrical and velocity fields, which leads to poor sensor performance. In the worst-case scenario, a strong irregularity can cause the electrodes to come so close that the breakdown voltage is exceeded, and a short circuit occurs. From this point on, no statement can be made about the measurement signal and the measurement electronics are prone to damage.

#### *Assembly*

Assembly of the sensor (protocol steps 3.4-3.6) is crucial, as this creates the electrode gap. As mentioned above, the distance between the electrodes is very important; this gap must be uniformly 1 mm over the entire length. These steps are important because they can change the electric field in the sensor drastically. The overall deposition behavior, as well as dendrite formation, can be influenced by the change in the electric field. Thus, it can no longer be guaranteed that the sensor response is linear to the incoming aerosol. The worst-case scenario of a short circuit also applies here.

## **Modifications**

### *3D printing*

Other possible modifications are the use of different 3D printing resins. There are many different resins on the market that can change the density, flexibility, temperature resistance, and strength of the sensor housing.

### *Sensor dimensions*

The first design criterion for the sensor is a safety configuration. The dielectric strength of air between the electrodes is 3 mm/kV. This length must not be undercut in any case. The higher the electric potential, the more particles are deposited, and these deposited particles are then prone to form dendrites. The dimensions of the electrodes were chosen so that easily available standard components can be used. Designs of similar sensors known to the authors used the following dimensions for a flat sensor: 9 mm width, 2 mm length, 1 mm gap, and 15 mm length, with a diameter of 8.5 mm and gap of 1.3 mm for a cylindrical design<sup>12,13</sup>. In addition, it should be ensured that the sensor can be manufactured by hand in a normal workshop. A 1 mm gap is the absolute minimum gap that still allows the sensor to be cleaned manually. Here, 1 kV was used as a good compromise of safety and efficient particle deposition, as well as availability of voltage sources in this range.

### *Electrodes*

Since the exact distance of 1 mm between the sensor electrodes is so crucial for performance, even more development work can be put into this step. For example, the 3D printed fixture can be made even more accurate, or a lathe can be used instead of a simple pipe cutter for cutting and deburring, if the equipment is available. Another option is to use a saw instead of a pipe cutter. In this case, the edges of the saw must be ground afterward. This

method causes less deformation than the pipe cutter, but takes longer. In comparison to epoxy glue, silicone gives the cables more room to move, and it becomes easier to respace the electrodes. However, since the cables have more room to move, it is more difficult to seal the sensor. Instead of the vacuum clamp, which is easier to open at once, a self-made design is also feasible. Here, only holes for some screws and a cavity for the sealing cord must be altered in the 3D design.

### *MFC*

The MFC determines how much of the aerosol is sucked through the sensor; the rest should be able to be drained through an overflow with a HEPA filter placed at the end of the overflow, to avoid pollution of the room. By choosing a less expensive pump instead of an MFC, higher flow fluctuations will influence the sensor signal negatively.

### *Dilution bridge*

As seen in **Figure 9**, a dilution bridge can be built with a simple needle valve parallel to one or more HEPA filters. Other designs include a small vise to squeeze the tube instead of the needle valve. This design has the advantage that the tube can be cleaned more easily. The more coils such a vise has, the finer the concentration can be adjusted. This is especially important for calibration measurements, where high dynamics should be avoided.

### *Bench multimeter*

The bench multimeter measures a voltage, which must be divided by the value of internal resistance to obtain the correct current value. Depending on the chosen measuring range (e.g., 100 V), this internal resistance value can vary (e.g., 1 M $\Omega$ ). It is important to select a defined range so that the internal resistance value is the same for all measured values.

If "auto range" is chosen, the internal resistance value must be tracked as well.

## **Troubleshooting**

### *3D printer*

If the printer stops, the tank should be checked for residues of the last print; the mixer often gets stuck. One should observe the first minutes of the printing process. If it is clogged, it is either because the correct slicer settings have not been set or the fresh print has not been stored under UV protected conditions before post-processing. In the slicer settings, no support points should obstruct the flow channel and the space between the electrodes, and the internal support structures box must be unlocked before sending the file to the printer.

### *Aerosol source + dilution bridge*

If the aerosol source seems unstable, all the HEPA filters should be checked to ensure they are in the correct position and are not clogged. Also, the aerosol generator as well as the reference instrument should be checked to ensure they have finished their warm-up phase.

### *Sensor*

The most common faults are caused by an insufficient power supply connection, an air leak at the sensor, or when deposited particles form soot bridges between the electrodes. First, the sensor is opened to check if soot bridges have formed between the electrodes. The power source must be turned off before disconnecting the sensor cables and opening the sensor. Soot bridges are easily visible to the naked eye and can be removed with little effort. To remove soot bridges, it is best to use an optical cleaning cloth or lint-free cotton swab.

A leak that changes the flow behavior in the sensor, as well as a lower voltage at the electrodes, can change the sensor

signal. It is not possible to say in advance which of these problems is responsible for an unexpected sensor response. Therefore, it is important to check both the tightness and the voltage stability as follows. First, connection from the cable to the electrodes is checked (protocol step 4.4). Next, the voltage source is checked to see if it is delivering the expected volts. An air leak is best identified with leak spray. In addition to this, the tightness can also be checked with a vacuum pump, as described in protocol step 4.4.2.

### Limitations

The limitation of an electrostatic sensor is well described by Maricq et al.<sup>14</sup>. In their work, they emphasize the importance of a stable voltage source and a stable sensor flow for the performance of the sensor. For this reason, a setup with an MFC or a pump should always be used for flow control, as described in **Figure 10**. In addition, the sensor needs a longer time to reach equilibrium during the first test. In further experiments, where a stable dendrite population has settled on the electrodes, the amount of time to start up the sensor is reduced. However, it should be generally noted that the sensor always needs a startup time to become operational depending on the initial concentration.

Unlike a flat design, as in Bilby et al., sensor drift is not a major problem in this cylindrical arrangement<sup>12</sup>. However, fast concentration changes at low particle concentrations are still difficult to detect with the sensor. As indicated by Diller et al. and Maricq et al., for a meaningful measurement signal, the measured value is averaged over 2-10 min, depending on how much the flow changes in the experiment<sup>14, 15</sup>.

With a slope of 2.8 nAm<sup>3</sup>/mg and a standard deviation of  $\pm 1.4$  nA, the deviation from the regression line in **Figure 11** is high. For a better understanding of the sensor accuracy, the comparison of several experiments is recommended.

For repeated experiments, the slope accounts for 3.5 nAm<sup>3</sup>/mg with a standard deviation of  $\pm 1.0$  nA, and 4.9 nAm<sup>3</sup>/mg with a standard deviation of  $\pm 0.6$  nA. In addition, the sensor will give a very high reading the moment the voltage source is switched on. This start value is filtered out of the measurement data.

The advantage of the method presented here lies clearly in the simplicity, but also in the versatile possibilities to adapt the sensor shape to different needs. Therefore, in addition to soot, the sensor can detect a large variety of charged particles and is suitable for a wide range of applications, for example, particulate matter detection from power plants, wildfires, industries, and automobiles. This paper should be an incentive to agencies, companies, research teams, citizen scientists, and anyone interested in the detection of particulate matter to reproduce this simple sensor construction manual and build their own particle detector.

### Disclosures

The author is employed by Silicon Austria Labs and is a student of the Technical University Graz. There are no other conflicts of interest to declare.

### Acknowledgments

This work was funded by the COMET Centre "ASSIC-Austrian Smart Systems Integration Research Center". ASSIC is co-funded by the BMK, the BMDW, and the Austrian provinces of Carinthia and Styria within the COMET-Competence Centres for Excellent Technologies programme of the Austrian Research Promotion Agency (FFG).

### References

1. World Health Organization. *Health Effects of Particulate Matter: Policy Implications for Countries in Eastern Europe, Caucasus and Central Asia*. (2013).
2. Giechaskiel, B. et al. Review of motor vehicle particulate emissions sampling and measurement: From smoke and filter mass to particle number. *Journal of Aerosol Science*. **67**, 48-86 (2014).
3. Giechaskiel, B. et al. Measurement of automotive nonvolatile particle number emissions within the European legislative framework: a review. *Aerosol Science and Technology*. **46** (7), 719-749 (2012).
4. Bainschab, M. et al. Measuring sub-23 nanometer real driving particle number emissions using the portable DownToTen sampling system. *Journal of Visualized Experiments*. (159), e61287 (2020).
5. Wang, X. et al. A novel optical instrument for estimating size segregated aerosol mass concentration in real time. *Aerosol Science and Technology*. **43** (9), 939-950 (2009).
6. Axmann, H., Bergmann, A., Eichberger, B. Measurement of ultrafine exhaust particles using light scattering. In *2013 Seventh International Conference on Sensing Technology (ICST)*. IEEE. 937-941 (2013).
7. Bermúdez, V., Luján, J. M., Serrano, J. R., Pla, B. Transient particle emission measurement with optical techniques. *Measurement Science and Technology*. **19** (6), 065404 (2008).
8. Michelsen, H. A., Schulz, C., Smallwood, G. J., Will, S. Laser-induced incandescence: Particulate diagnostics for combustion, atmospheric, and industrial applications. *Progress in Energy and Combustion Science*. **51**, 2-48 (2015).
9. Giechaskiel, B., Cresnoverh, M., Jörgl, H., Bergmann, A. Calibration and accuracy of a particle number measurement system. *Measurement Science and Technology*. **21** (4), 045102 (2010).
10. Kulkarni, P., Baron, P. A., Willeke, K. *Aerosol Measurement: Principles, Techniques, and Applications*. Wiley. Hoboken, NJ. (2011).
11. Agarwal, J. K., Sem, G. J. Continuous flow, single-particle-counting condensation nucleus counter. *Journal of Aerosol Science*. **11** (4), 343-357 (1980).
12. Bilby, D., Kubinski, D. J., Maricq, M. M. Current amplification in an electrostatic trap by soot dendrite growth and fragmentation: Application to soot sensors. *Journal of Aerosol Science*. **98**, 41-58 (2016).
13. Warey, A., Hall, M. J. Performance characteristics of a new on-board engine exhaust particulate matter sensor. *SAE Transactions*. **114** (14), 1489-1497 (2005).
14. Maricq, M. M., Bilby, D. The impact of voltage and flow on the electrostatic soot sensor and the implications for its use as a diesel particulate filter monitor. *Journal of Aerosol Science*. **124**, 41-53 (2018).
15. Diller, T. T., Hall, M. J., Matthews, R. D. Further development of an electronic particulate matter sensor and its application to diesel engine transients. *SAE Technical Paper*. (2008).